CHAPTER 3
RESULTS

This chapter examines the coupling efficiency in terms of its accuracy within the tracking volume, applied forces to the patient when coupling and drilling, as well as robot stiffness and its influence on the surgical procedure. The experiments were performed using the KUKA LBR3 and these results apply only to this particular robot arm. Further extensive testing should be made to use the developed prototype with other robotic arms and under patient surgery.

3.1 IMAGE PROCESSING TRACKING ERRORS

3.1.1 DEPTH ERROR

This error refers to the distance error between the camera plane and the centre of the target plane (blue plane and red planes on Figure 63 respectively). The depth, or distance to target error was plotted as a cumulative frequency graphic (37) and presented in Figure 73.

The actual calculated values and cumulative percentage tables are presented in Appendix B and Appendix E.

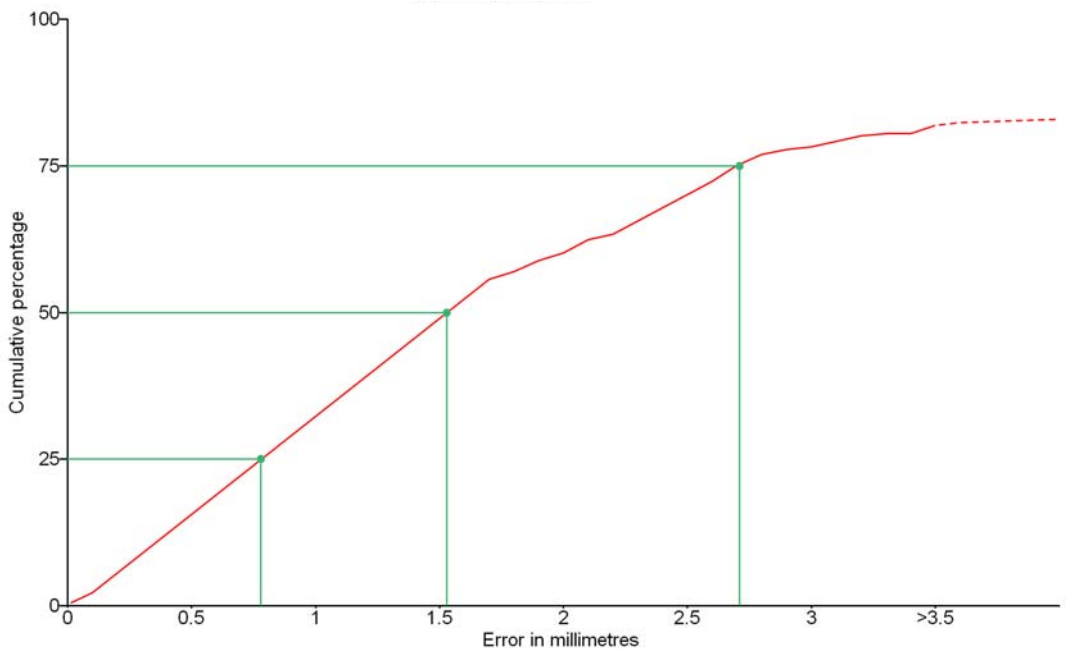

Figure 73 - Cumulative depth error within the tracking volume. Horizontal axis contains the error magnitude in millimetres. Vertical axis contains the cumulative percentage of the error.

Analysing the obtained results it is observed that:

- The depth median error within the tracking volume is 1.53mm.
- The lower and upper quartile errors are 0.78mm and 2.71mm respectively. The interquartile range is therefore 1.93mm.

In order to perceive the spatial distribution of this error, the 221 collected points are depicted in the following figure, and are characterized by individual arrows representing the normal of the image sensor plane, together with its relationship to the centre of the target. The colour of the arrow represents the magnitude of error in that position with that viewing angle.

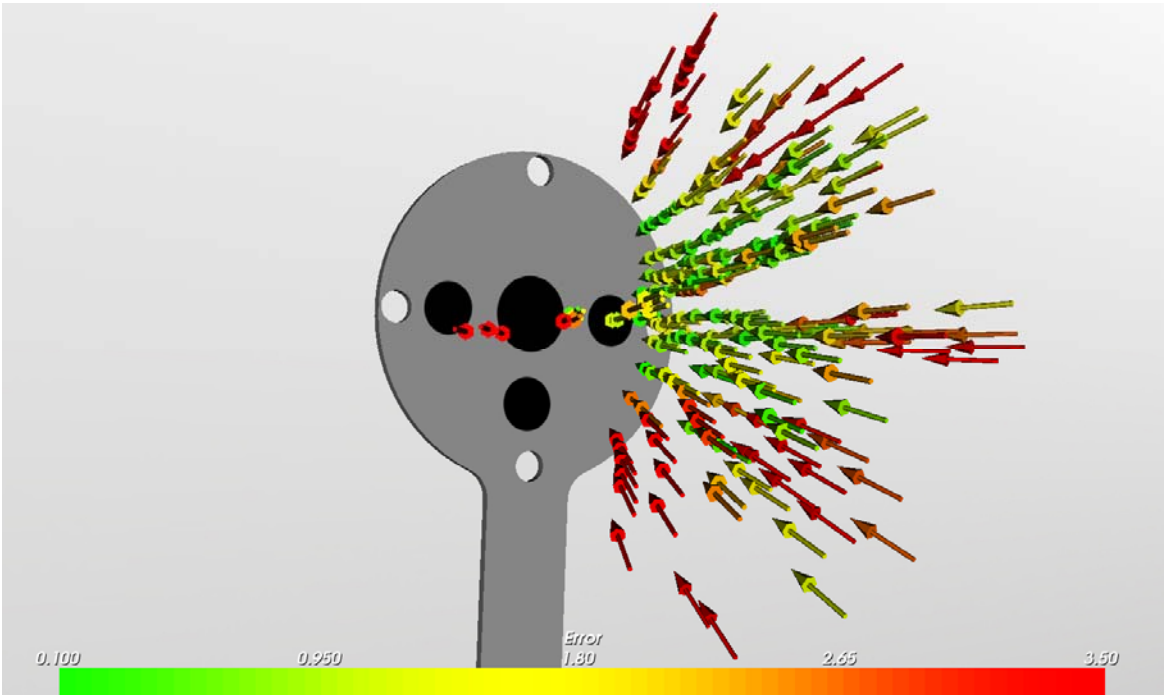

Figure 74 - Spatial representation of the depth error growth with the camera distance and orientation.

The analysis of Figure 74 shows that:

- The normal vector from the target plane contains the lesser error, in the range of 0.1mm, where as the points further away from this path and tilted regarding the target plane can go over to 3.5mm.
- Tilting the camera slightly from this axis results in an immediate error increase.

3.1.2 COPLANAR ANGLE ERROR

To calculate the coplanar angle error, the tilt of the camera housing was calculated with the intersection of the two housing planes. The angle between this line and the horizontal line defined in the tool plane is compared with the image processing information, and the coplanar angle error is calculated (Figure 75). The actual calculated values and cumulative percentage tables are presented in Appendix C and Appendix F.

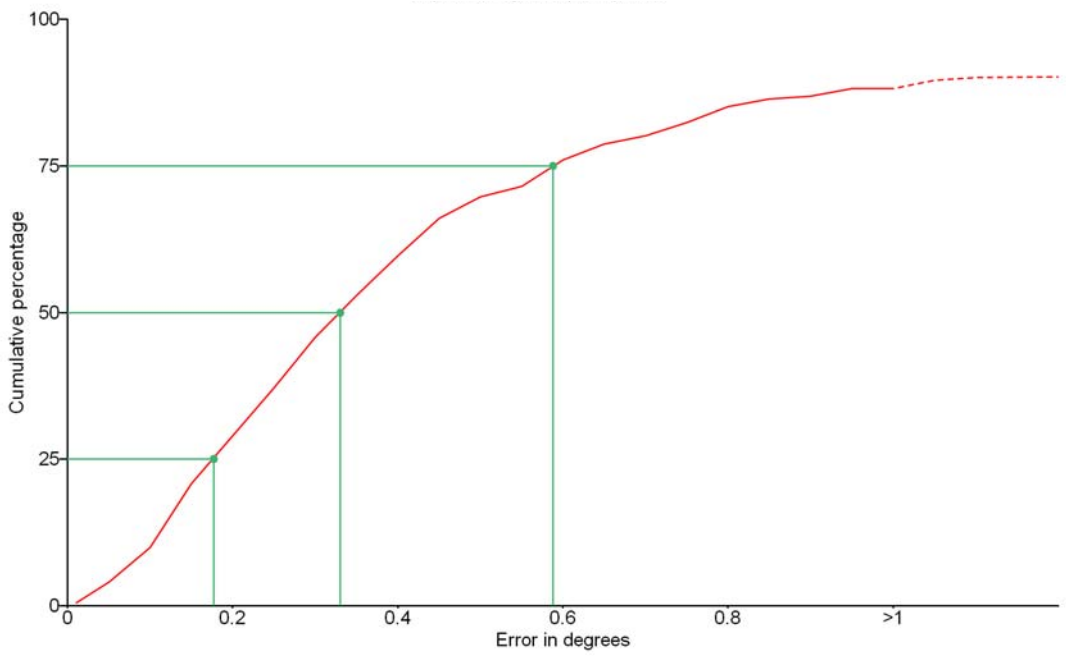

Figure 75 - Cumulative coplanar angle error within the tracking volume. Horizontal axis contains the error magnitude in degrees. Vertical axis contains the cumulative percentage of the error.

Analysing the calculated errors it is observed that:

- The coplanar angle median error within the tracking volume is 0.33º.
- The lower and upper quartile errors are 0.177º and 0.588º respectively. The interquartile range is therefore 0.411º.

Akin to the depth error, the spatial distribution of the coplanar angle error is represented in Figure 76. The errors are characterized by same prior individual arrows. The colour of the arrow represents the magnitude of error in degrees from that position with that viewing angle.

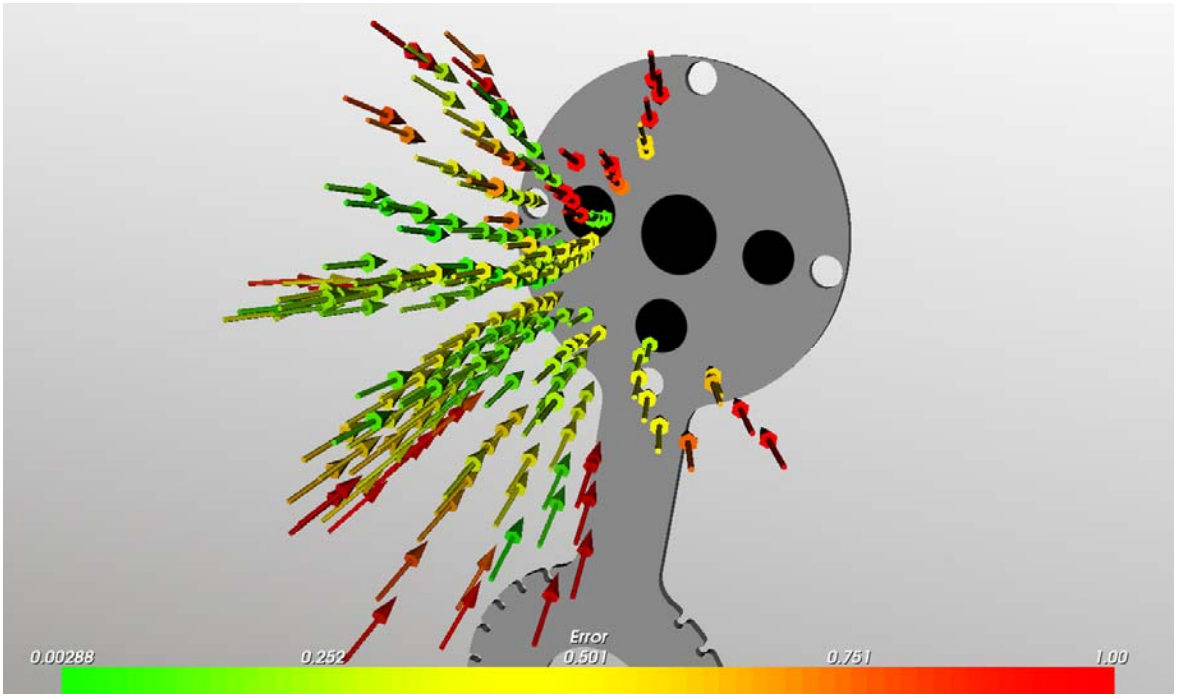

Figure 76 - Spatial representation of the angle error growth with the camera distance and orientation.

From Figure 76 it is observed that:

- The coplanar angle shares the same characteristics as the measured inaccuracies of depth.
- The normal vector of the target plane has the lowest error, 0.1º, while higher error over 1º can be found in extreme positions of the tracking volume.
- The angle error does not grow as fast when tilting the camera from the target normal vector, as does the depth error.

3.1.3 XY POSITION ERROR

This error refers to the image sensor plane in relationship to the target plane. This positioning in XY image sensor plane coordinates is then converted into millimetres with the relationship px mm equation mentioned in Chapter 2 - Equation 7. The cumulative frequency graphic is presented in Figure 77. The actual calculated values and cumulative percentage tables are presented in Appendix D and Appendix G.

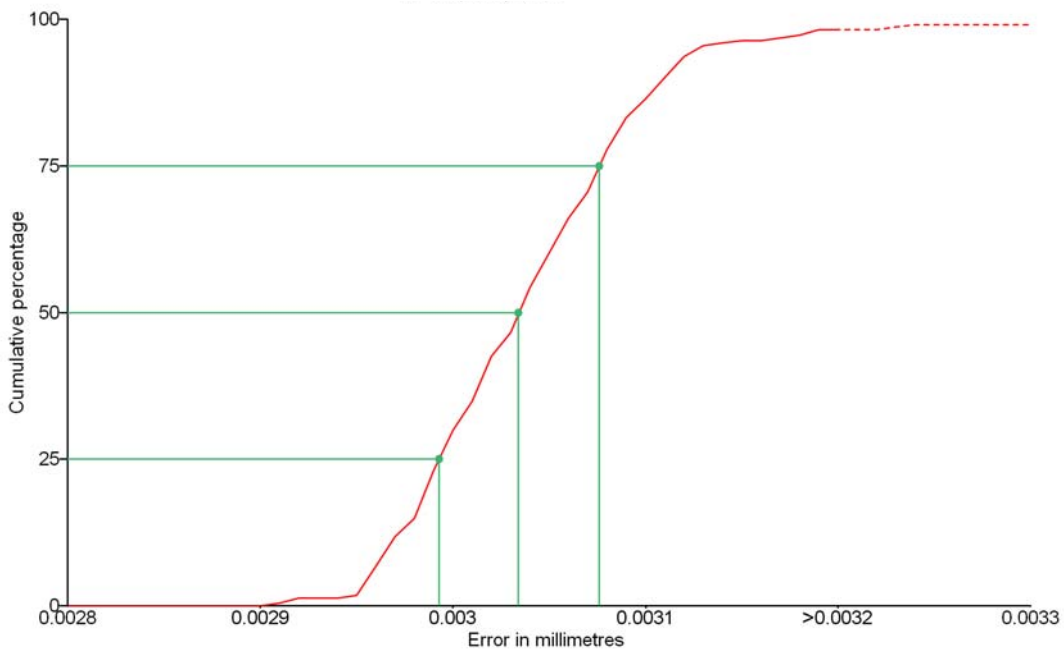

Figure 77 - Cumulative XY position error within the tracking volume. Horizontal axis contains the error magnitude in millimetres. Vertical axis contains the cumulative percentage of the error.

Analysing the calculated errors it is observed that:

- The XY position median error within the tracking volume is $30.34e^{-4}$mm.
- The lower and upper quartile errors are $29.93e^{-4}$ mm and $30.76e^{-4}$ mm respectively. The interquartile range is therefore $8.3e^{-5}$ mm.

Figure 78 depicts the error growth for X and Y depending on the camera position and orientation relative to the target. Contrary to the previous calculated errors, the FaroArm information was only used to know which points in space produce which error.

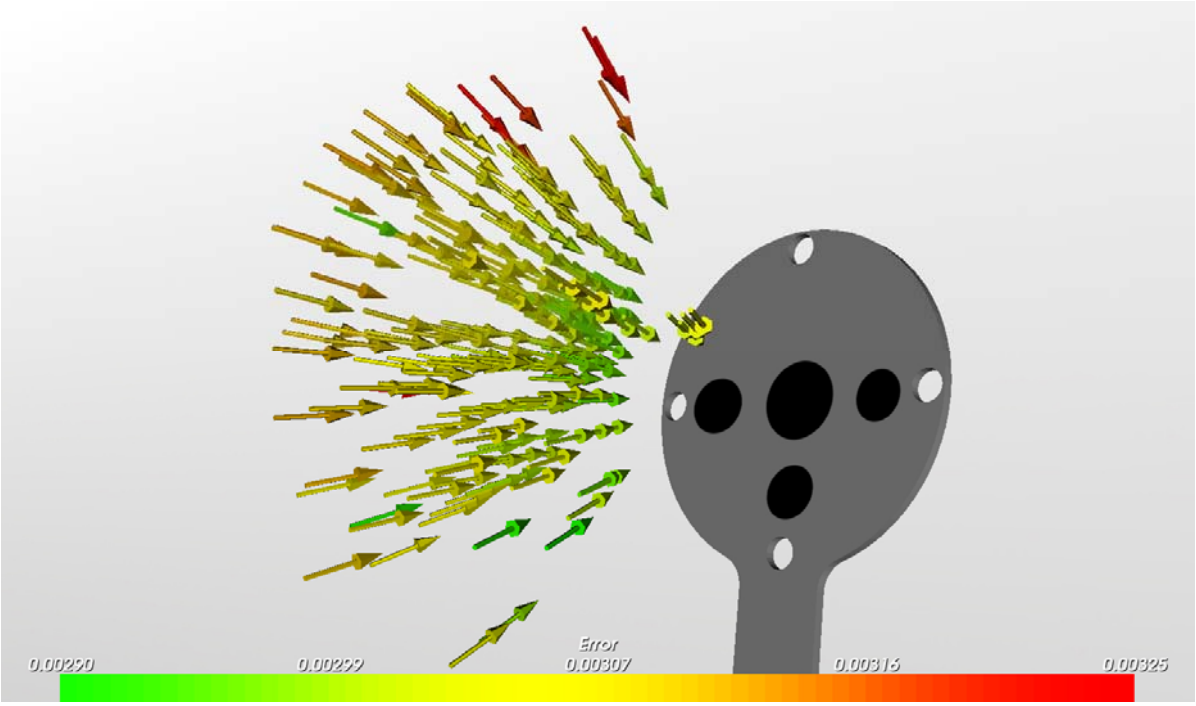

Figure 78 - Spatial representation of the XY plane position error growth with the camera distance and orientation.

From Figure 78 it is observed that:

- The calculated errors range between $2.8e^{-3}$ mm to $3.25e^{-3}$ mm, being the lowest error achieved when the camera is closer to the target.
- Tilting the camera in relationship to the target has little influence on this error.

3.2 COUPLING BETWEEN ROBOT ARM AND TOOL

The hypothesis presented in this thesis is the possibility to couple a moving robot and a patient-bound tool without exerting forces on the patient. To detect if the coupling has been successful in achieving this goal, the forces must to be measured on the end of the surgical tool as if they would be felt by the patient.

During the coupling procedure the values of the FTS and the robot position were displayed and recorded. In the following figure the results of the coupling procedure are presented:

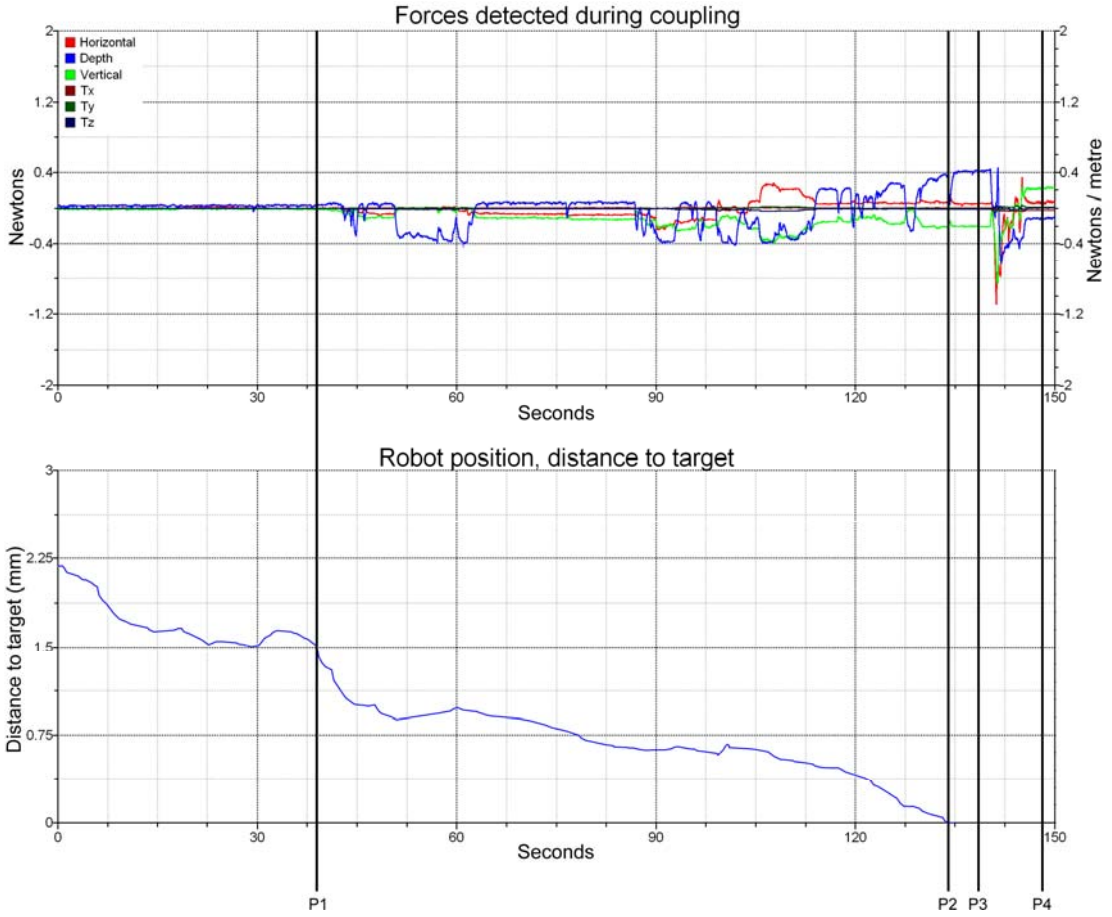

Figure 79 – Top: Detected forces by the FTS. Bottom: Distance from the target as indicated by the robot controller. Horizontal axis displays time in seconds. On the top graphic the vertical axis contains the measured force in Newton as well as the torques in Newton / metre, the bottom graphic the distance to the target in millimetres.

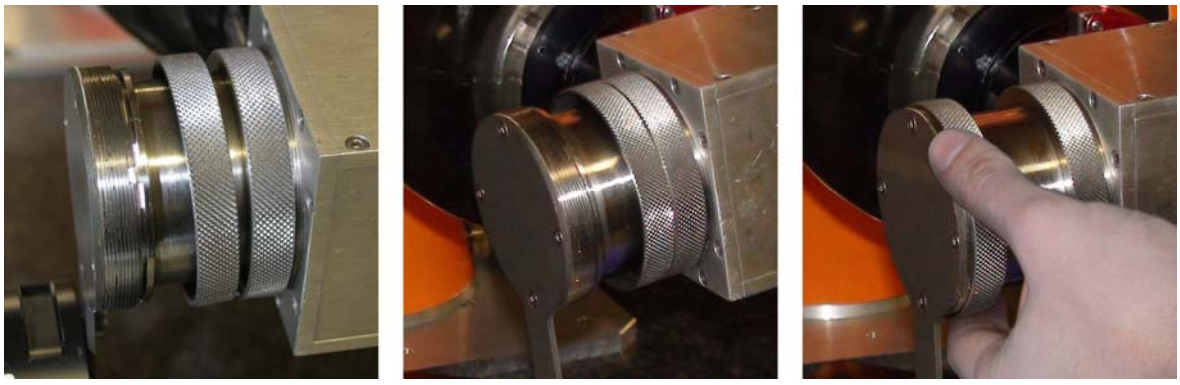

Figure 80 - From left to right: P1, P2 and P3 in the coupling sequence.

From this experiment it is observed that:

- At point P1, 1.5 mm from the end position, the robot is already inside the coupling device and no forces are detected (Figure 80, left photo).
- As the robot proceeds further, between P1 and P2, minor forces are detected as the pieces brush each other during coupling. The maximum detected force is 0.4N, the equivalent to 39.2gramms

- At point P2 the robot achieves the coupled status with the surgical tool (Figure 80, central photo).
- Between points P3 and P4, the fixation rings are rotated (by hand) to secure the design. When doing so higher forces are applied to the tool, which can go over to 2N. These forces are not applied by the robot, but by the surgeon when manipulating the device and fastening the pieces (Figure 80, right photo).
- The detected torques were minimal and reached a maximum of -0.035N/m throughout the experiment.

3.3 LIGHT-WEIGHT ROBOT STABILITY IN MAINTAINING POSITION DURING LOAD

Once coupling has been achieved, the next stage of the surgical workflow involves holding the target position while the surgeon continues his task. This requires that the robot remains stable with different loads being applied during surgery. Given the characteristic stiffness of the light-weight robots, two types of measurements were conducted to evaluate their possible use in surgery. One experiment with a static load being applied and dynamic load which forces the robot to react quickly while maintaining the same target position.

3.3.1 WITH STATIC LOAD

The researcher applied a constant manual force between 1 to 2Kg and the position oscillation was measured with the robot's internal encoders. The amount of force was estimated with a gross hand push on a scale, the repeatability of the exact same force is naturally unattainable. Firstly the robot is pressed downwards for a few seconds and sequentially upwards. Secondly, back and forth and finally a force is applied from the left to the right. Figure 81 illustrates the result of this experiment.

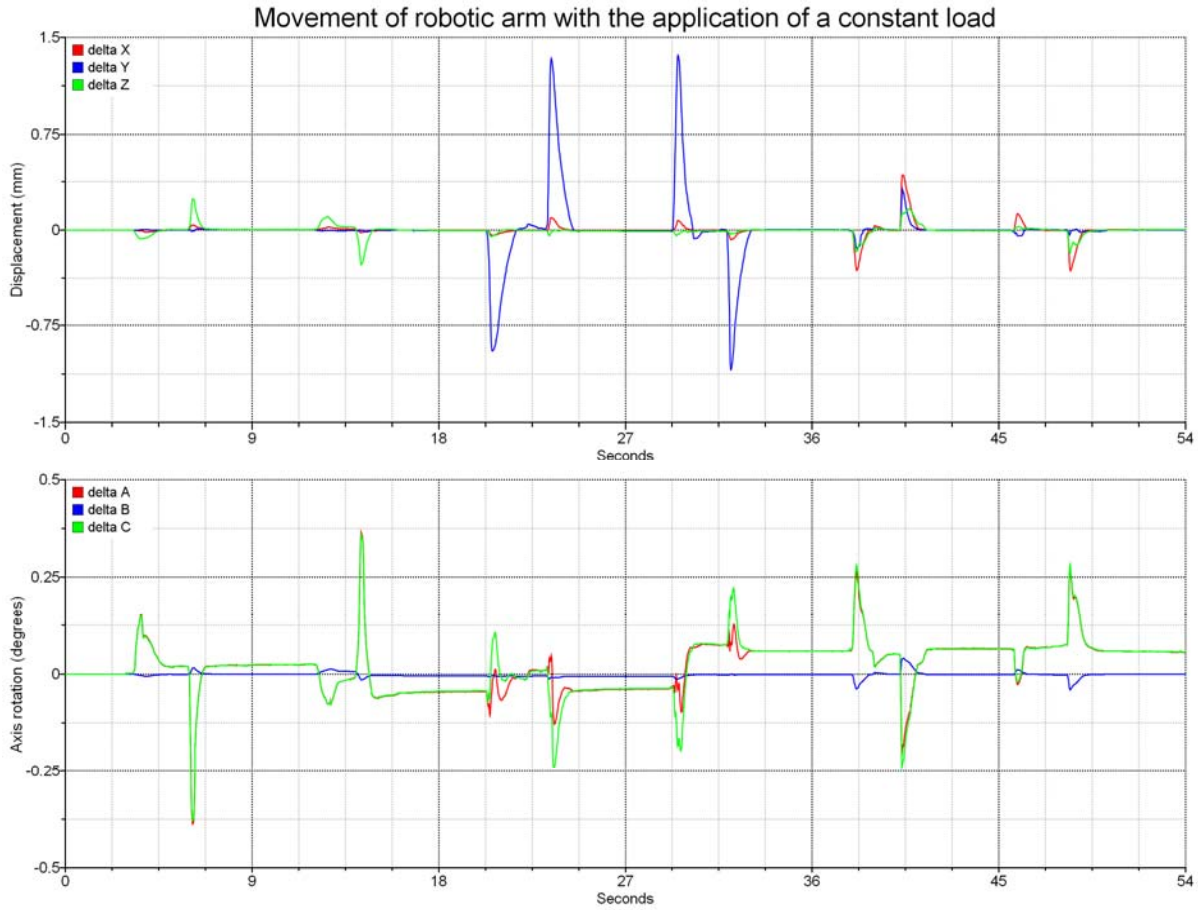

Figure 81 - Top: Position oscillation with constant load applied. Down: Angle oscillation with constant load applied. Horizontal axis displays time in seconds. On the top graphic the vertical axis displays the robot arm displacement in millimetres, the bottom graphic the robot arm displacement in degrees.

From this experiment it is observed that:

- From 0 to 9 seconds, the robot is pressed downwards and the obtained reaction is the robot arm follows the force displacing the target position by -0.069mm before repositioning itself into the original position.
- Upon release the robot overshoots the original position by 0.25mm before resuming the original position.
- During the same period angles A and C also presented similar behaviour. Being displaced 0.16º when pressing down and -0.4º upon release.
- It took slightly more than one and a half seconds before recovering the original position. Likewise for the release and consequent overshoot.
- From 9 to 18 seconds the applied force was again on the Z axis but upwards. Similar behaviour was encountered with slightly larger displacements.
- Both A and C angles reported a 0.025º difference after the pressure was release. This offset error remained until another force was applied to the robot. Between 9 and 18 seconds and the robot arm being pressed upwards the offset error turned into -0.05º.

- Between seconds 18 and 27 the robot was pressed forward in depth towards the target. This force made the robot arm displace approximately 1 millimetre.
- The constant force in this direction was more unstable and did not stabilize again in zero like downwards. Upon release the Y position overshoot by 1.35mm.
- Applying the same force in the opposite direction resulted in the mirrored result (between 27 and 36 seconds).
- During the period of 18 and 36 seconds, the rotation error of axis A and C oscillates between -0.25º to 0.25º and finishes with 0.06º of error from the original position.
- Between 36 and 54 seconds the applied force was horizontal and displaced the robot arm in all three directions by approximately between -0.35mm and 0.45mm. During this period the X axis the one which suffered the most displacement.
- During the same period the angle error oscillates between 0.25º and -0.25º, again under the A and C axis.
- The repeated behaviour observed during the 54 seconds is that with a constant load being applied in one axis, the robot compensates the movement within one and a half seconds. However upon release the overshoot takes the complementary direction, often with higher displacement that the original.
- An additional remark is that throughout the experiment the angle error not only reflects the position behaviour, but maintains a hysteresis and error offset of 0.06º upon release of the constant load.
- The most sensitive axis to an external force is the Y, or depth axis. The most resistant is the X or the vertical axis.

3.3.2 WITH DYNAMIC LOAD

With the same experimental setup a dynamic load was applied. Here the researcher applied a force in one direction and quickly change directions under the same axis of the applied force. The amplitude of this force is estimated to be 2Kg, and the frequency approximately half a Hertz. The applied force has therefore a sinusoid shape. The results are presented in Figure 82.

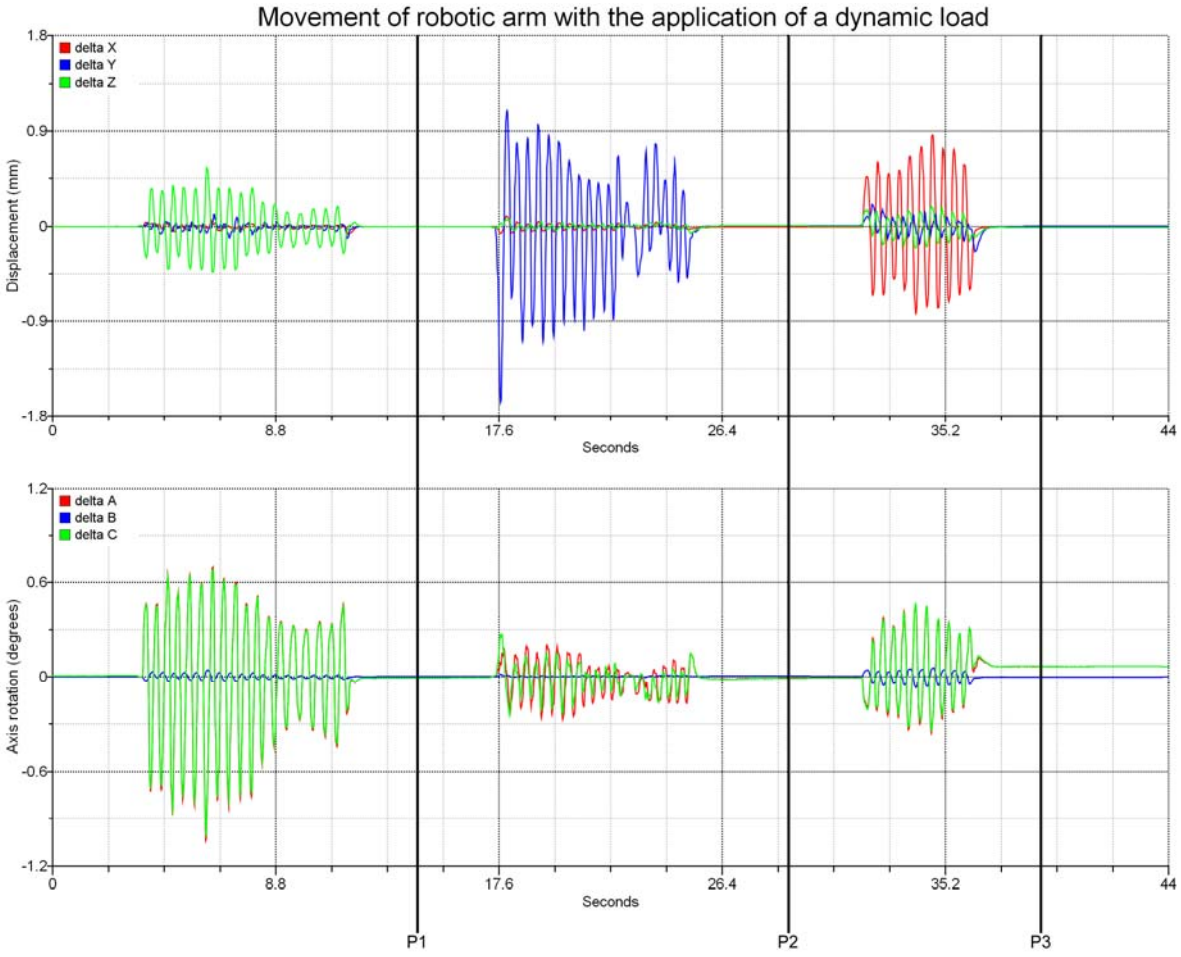

Figure 82 - Top: Position oscillation with dynamic load applied. Down: Angle oscillation with dynamic load applied. Horizontal axis displays time in seconds. On the top graphic the vertical axis displays the robot arm displacement in millimetres, the bottom graphic the robot arm displacement in degrees.

From this experiment it is observed that:

- From 0 to P1, the robot is subjected to forces from above and below with a 0.42 frequency, the position variation amplitude was of 0.9mm.
- During the same period angles A and C oscillated with amplitudes between 1.45º and 0.576º.
- Between P1 and P2 the robot was pressed in depth and this resulted in amplitude variation between 2.3mm and 1.3mm in that axis.
- Both A and C rotation angles oscillated between 0.48º and 0.238º in this period.
- From P2 and P3 the force was applied laterally and the resulting axis X oscillated between 1.55mm and 1.1mm
- Similarly angles A and C oscillated around 0.695º.
- The repeated behaviour observed during this experiment is that with a dynamic load produces movement of the target which can not be absorbed by the light weight robot. Both position and angle errors share the same behaviour with the

addition that the angle error is not fully corrected when external forces stop being applied.

- The most sensitive axis to an external force is the Y, or depth axis. Contrary to the constant load experiment, the most resistant is the Z or the horizontal axis.

3.4 STABILITY DURING DRILLING OF THE MAXILLA ON A PHANTOM PATIENT

In Figure 83 the results of the drilling process are illustrated.

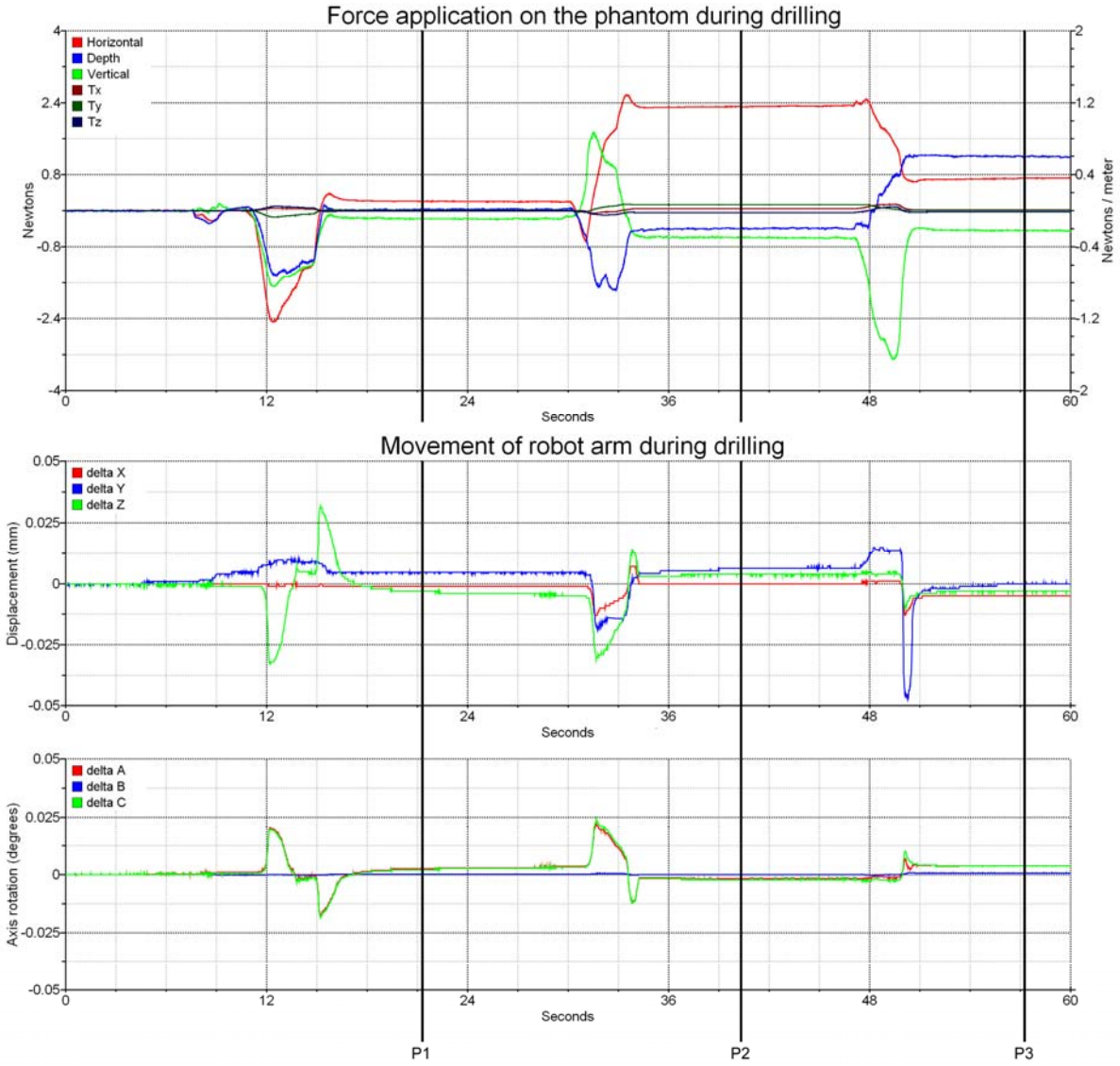

Figure 83 - Robot position oscillation and applied forces during drilling of the phantom's maxilla. Horizontal axis displays time in seconds. On the top most graphic the vertical axis displays measured forces in Newton as well as the torques in Newton / metre. The central graphic displays the robot arm displacement in millimetres, the bottom graphic the robot arm displacement in degrees.

From this experiment it is observed that:

- From 0 to P1, a hole was drilled vertically which resulted in an initial displacement of 0.033mm downwards. This displacement was compensated by the robot arm, and upon removal of the drill a position overshoot of 0.03mm was again observed.
- During this period angles A and C displaced 0.02º with same magnitude overshoot upon release.
- The forces measured in this position exceeded 2.4N, or 235.2g, predominately on the same axis as the robot arm mostly displaces.
- Between P1 and P2 one lateral hole was drilled which resulted in a displacement in the vertical (Z) axis of 0.03mm.
- Upon release of this force, the robot did not return to the exact same position, but presented a constant displacement of approximately 0.007 in the depth axis (Y) and 0.0045mm in the horizontal X axis.
- This displacement produced a extra force on the tool of 2.4N, or 235.2g, which remained until the robot was again displaced by the drilling procedure of the third hole.
- During this period the angular deviation was similar to the period 0 to P1.
- Additionally the overshoot of both position and orientation was considerably lower than previously observed.
- Between P2 and P3 a third drill hole was made in the opposing lateral wall of the phantom's maxilla. This resulted in a displacement of 0.015mm in the direction of the target (depth, Y).
- The observed overshoot of the position was considerably higher, approximately -0.05mm.
- A residual offset of 0.005mm and 0.0042º at the end of the experiment was observed.
- The overall behaviour observed during this experiment is that drilling the phantom resembles the application of a constant load on the robot arm. Overshoot of the position upon release of the force and remaining target position offset of approximately 0.005mm and 0.06º (in the case of the constant load experiment)
- The most sensitive axis to an external force is the Y, or depth axis.

3.5 STABILITY DURING DRILLING AND SCREW FIXATION ON A SWINE SKULL

Since the plastic skull is softer than bone, further testing with a swine skull bone was performed. This helped to better understand the behaviour of this light weight robot under more realistic conditions.

3.5.1 POSITION STABILITY DURING DRILLING

The measured position deviation during the drill procedure of the swine skull is presented in Figure 84.

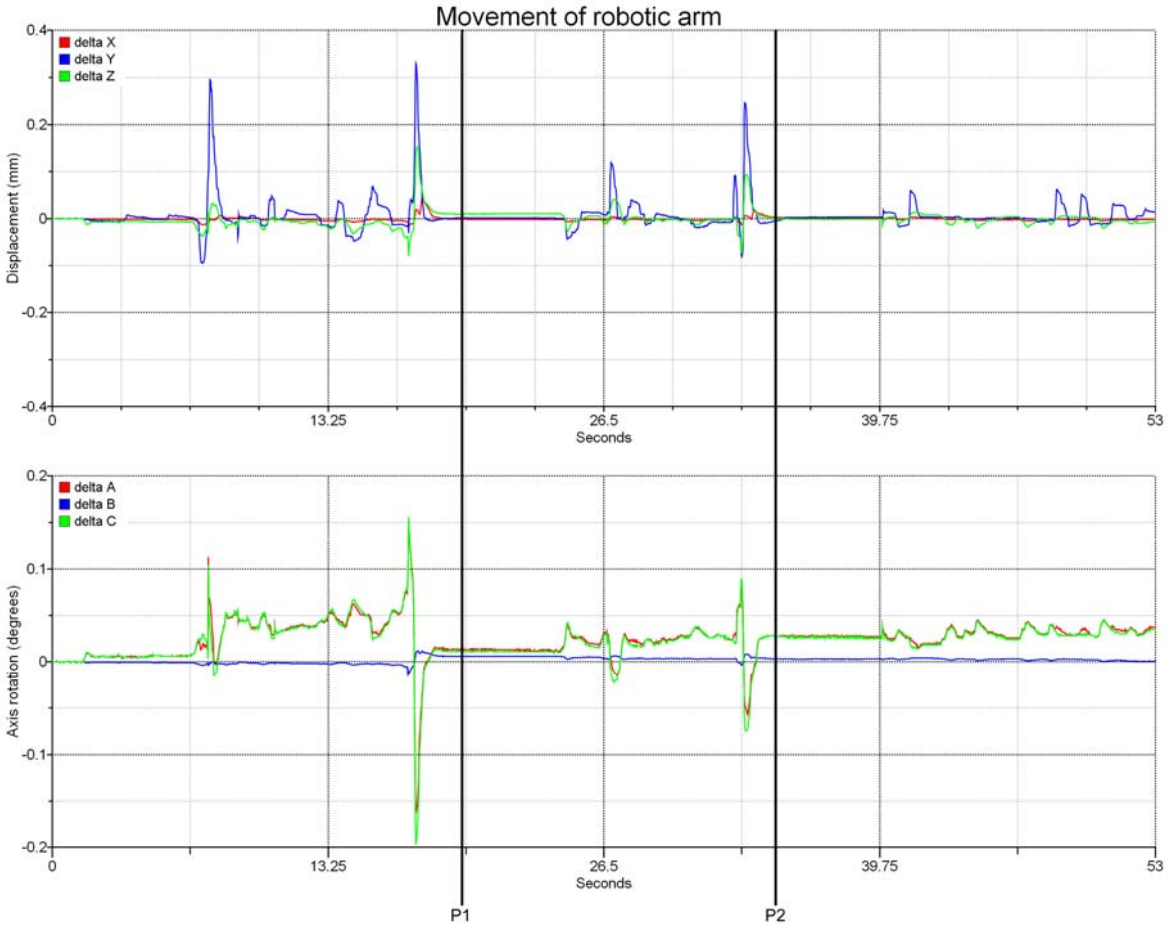

Figure 84 - Robot arm position during drilling of the swine bone. Horizontal axis displays time in seconds. On the top graphic the vertical axis displays the robot arm displacement in millimetres, the bottom graphic the robot arm displacement in degrees.

From this experiment it is observed that:

- From 0 to P1, one hole was drilled until the drill bit pierced the bone and reached the nasal cavity. This resulted in a displacement towards the surgical tool. This displacement spiked twice with amplitudes of 0.3mm and 0.33mm respectively.
- The two displacement spikes lasted for 0.76 and 0.74 seconds.
- During the same period angles A and C suffered similar displacements oscillating between 0.155º to -0.2º together with the second Y (depth) displacement spike.
- Between P1 and P2 a second hole was drilled which provoked a displacement spike of 0.25mm and -0.08º.
- After the second drill hole, the orientation error offset was 0.029º. The position offset was approximately zero.
- Between P2 and the end of the experiment the third hole was drilled. During this period the robot oscillation reached a maximum of 0.06mm.

- The angle oscillation was lower than the remaining offset of the previous drill position.
- The overall behaviour observed during this experiment is that drilling the swine bone, contrary to the phantom, does not resemble the application of a constant load on the robot arm. A mix of both constant and dynamic forces is observed. The robot's ability to recover the original position after the application of these forces is recognized with the largest offset error being found in the rotation axis A and C.

3.5.2 POSITION STABILITY DURING SCREW FIXATION

Contact between the end effector and the surgeon was noted throughout the whole experiment, in particular when fixating the third screw, which presented some problems and did not grip easily. The surgeon rested his hand on the robot arm while pressing down and rotated the screw.

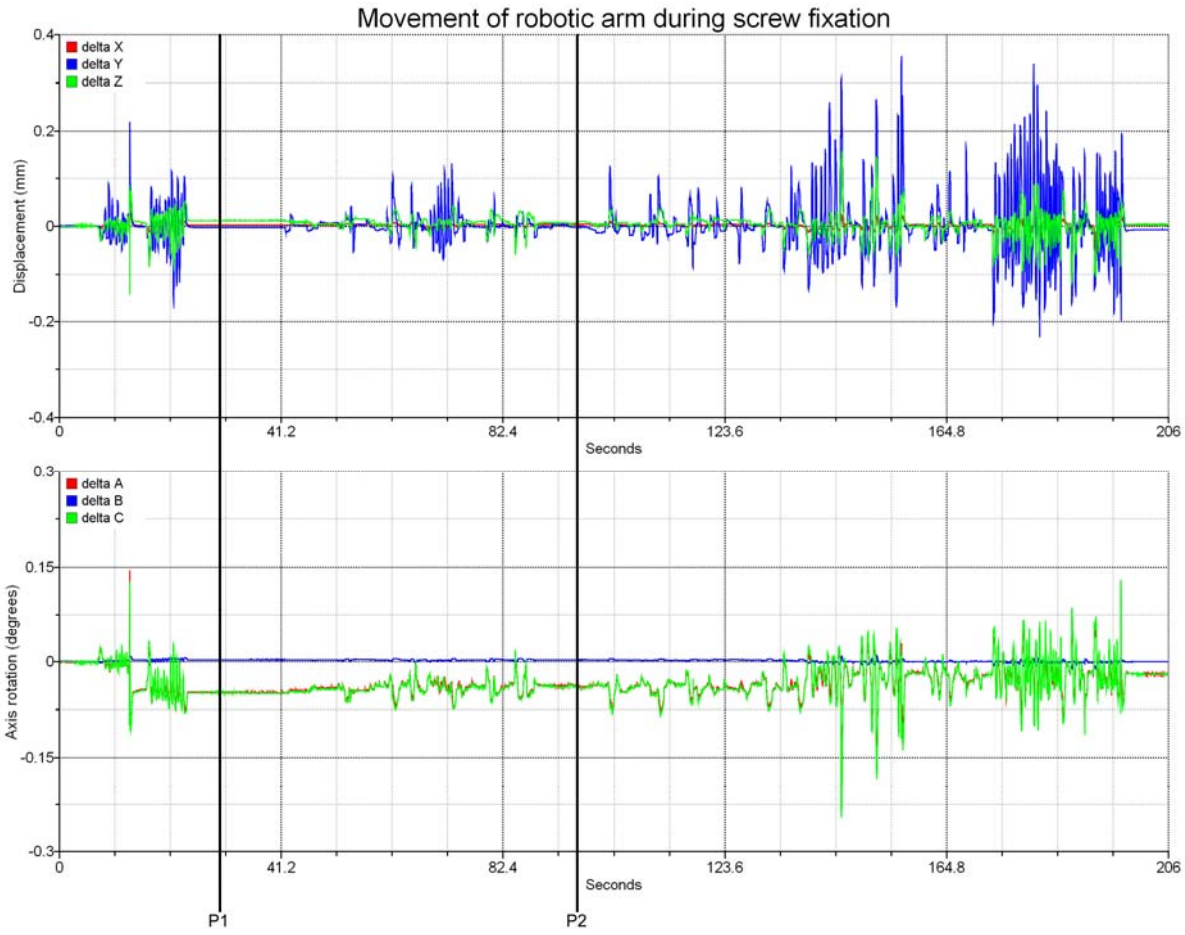

Figure 85 - Robot arm position during screw fixation of the swine bone. Horizontal axis displays time in seconds. On the top graphic the vertical axis displays the robot arm displacement in millimetres, the bottom graphic the robot arm displacement in degrees.

From this experiment it is observed that:

- From 0 to P1, one screw was inserted with forces oscillating at a frequency of 1.47Hz.

- The maximum displacement of the robot arm was 0.22mm and 0.15º.
- The offset of the robot arm at P1 was 0.013mm in the Z (vertical) axis and -0.05º.at both rotation axis A and C.
- Between P1 and P2 a second screw was inserted which resulted in similar oscillation as the previous screw, but with lower displacement amplitude, approximately 0.2mm.
- The rotation axis also suffered less oscillation and maintained the previous offset of -0.05º.
- From P2 to the end of the experiment, the third screw was inserted. The maximum displacement measured was 0.36mm on the depth (Y) axis, and -0.25º on both A and C rotation axis.
- After the screw had been inserted the offset from the original position was 0.005mm on the X and Z axis and -0.02º in the A and C angles.
- Similar to the drilling procedure the robot showed ability in recovering the original position after the application of these forces. As well as a remaining offset displacement is observed in both position and angle.